Clinical Immunology 284 (2026) 110665

Contents lists available at ScienceDirect

Clinical Immunology

journal homepage: www.elsevier.com/locate/yclim

Integrated single cell RNA sequencing and flow cytometry analysis identifies elevated S100A6^{+} and S100A8^{+} myeloid subsets in pancreatic ductal adenocarcinoma

Afshin Derakhshani [a,b,c,d,1], Roberta Di Fonte [e,1], Letizia Porcelli [e,1], Fatemeh Nejadi Orang [f,1], Mahdi Abdoli Shadbad [f,1], Adib Miraki Feriz [g,1], Hossein Safarpour [h,1], Antoine Dufour [a,b,c,d], Behzad Baradaran [f], Angela Calabrese [i], Mario Testini [j], Riccardo Memeo [k], Giovanna Di Meo [j], Leonardo Vincenti [l], Sonali Bhardwaj [b,d,m], Vito Racanelli [n], Nicola Silvestris [o,*], Oronzo Brunetti [p,2], Amalia Azzariti [e,2]

[a] *Calvin, Phoebe and Joan Snyder Institute for Chronic Diseases, Department of Microbiology, Immunology, and Infectious Diseases, Cumming School of Medicine, University of Calgary, AB, Canada*
[b] *McCaig Institute for Bone and Joint Health, University of Calgary, Calgary, Canada*
[c] *Department of Microbiology, Immunology, and Infectious Diseases, Cumming School of Medicine, University of Calgary, Calgary, Canada*
[d] *Department of Physiology and Pharmacology, University of Calgary, Calgary, AB, Canada.*
[e] *Experimental Pharmacology Laboratory, IRCCS Istituto Tumori Giovanni Paolo II, Bari, Italy*
[f] *Immunology Research Center, Tabriz University of Medical Sciences, Tabriz, Iran*
[g] *Wellcome Trust Sanger Institute, Wellcome Genome Campus, Hinxton, Cambridge, UK*
[h] *Cellular and Molecular Research Center, Birjand University of Medical Sciences, Birjand, Iran*
[i] *Radiology Unit, IRCCS Istituto Tumori Giovanni Paolo II, Bari, Italy*
[j] *Department of Precision and Regenerative Medicine and Ionian Area (DiMePre-J), University of Bari, Bari, Italy*
[k] *Department of HPB Surgery, Miulli Hospital, Acquaviva delle Fonti, Italy*
[l] *General Surgery Unit, National Institute of Gastroenterology IRCCS Saverio de Bellis, Research Hospital, via Turi 27, Castellana Grotte, 70013 Bari, Italy*
[m] *Department of Biochemistry and Molecular Biology, Cumming School of Medicine, University of Calgary, Calgary, Canada*
[n] *Centre for Medical Sciences, University of Trento and Internal Medicine Division, Santa Chiara Hospital, Provincial Health Care Agency (APSS), Trento, Italy*
[o] *Medical Oncology Unit - IRCCS Istituto Tumori 'Giovanni Paolo II', Bari, Italy*
[p] *S.S.D. C.OR.O, Bed Management, Presa in carico, Team Multidisciplinari, IRCCS Istituto Tumori 'Giovanni Paolo II', Bari, Italy*

ARTICLE INFO

Keywords:
Dendritic cells
Monocytes
Pancreatic neoplasms
Peripheral blood mononuclear cells
S100A

ABSTRACT

Pancreatic ductal adenocarcinoma (PDAC) is among the most lethal malignancies, underscoring the need for minimally invasive biomarkers to support patient stratification and disease monitoring. In this study, we aimed to identify PDAC-associated immune signatures by reanalyzing a single-cell RNA-sequencing dataset and to validate key findings using flow cytometry in an independent cohort predominantly composed of advanced-stage PDAC. Analysis of peripheral blood mononuclear cells from patients with PDAC and healthy donors revealed increased expression of S100A6, S100A8, and S100A12, particularly within monocytes and dendritic cells. These transcriptional changes were confirmed at the protein level, demonstrating enrichment of S100A6^{+} monocytes, S100A6^{+}/S100A8^{+} DCs, activated monocytes, and plasmacytoid DCs in PDAC. Univariate ROC analyses identified S100A6^{+} plasmacytoid DCs, S100A8^{+} plasmacytoid DCs, and CD14^{+}CD86^{+}S100A8^{+} monocytes as candidate PDAC-associated immune features. However, further validation incorporating benign pancreatic conditions and multivariable modeling is required before conclusions can be drawn regarding diagnostic specificity and clinical applicability.

* Corresponding author at: Medical Oncology Unit - IRCCS Istituto Tumori 'Giovanni Paolo II', Bari, Italy.
E-mail address: n.silvestris@oncologico.bari.it (N. Silvestris).
[1] These authors equally contributed
[2] Co-last authors

https://doi.org/10.1016/j.clim.2026.110665
Received 29 September 2025; Received in revised form 6 January 2026; Accepted 9 January 2026
Available online 21 January 2026

1. Background

Pancreatic ductal adenocarcinoma (PDAC) is a prevalent and aggressive form of pancreatic cancer, which is considered the third-leading cause of cancer-related deaths in both men and women [1]. Its incidence and mortality continue to rise globally, with estimates reaching 18.6 cases per 100,000 by 2050, underscoring its growing public health impact [2]. Despite remarkable advancements in our understanding of PDAC biology, the prognosis of affected patients is poor, owing to late-stage diagnosis, the occurrence of early metastasis, and the limited availability of treatment options [3]. These challenges underscore the urgent need for sensitive biomarkers to improve the detection and monitoring of PDAC, thereby improving patient management and clinical decision-making. A key hurdle lies in identifying and validating tumor biomarkers through minimally invasive approaches, such as liquid biopsy [4]. However, the detection of small amounts of tumor-specific molecules such as cell-free DNA, cell-free RNA fragments, tumor antigens, or exosomes in the body fluids of patients for cancer detection remains challenging, especially in early-stage cancer due to extremely low levels of tumor-specific molecules in the peripheral blood [5]; Carbohydrate antigen 19–9 (CA 19–9) seems to be one of the rare serum biomarker widely approved for the clinical management of such patients [6,7]. This protein is also relevant in other gastrointestinal, hepatopancreatobiliary, and extragastrointestinal cancers, with roles in diagnosis, prognosis, and surgical decision-making [8]. PDAC is characterized by immune dysfunction both within the tumor microenvironment (TME) and systemically. The TME shows multiple immune deficiencies, including reduced levels of functional $CD4^+$ and $CD8^+$ T cells. Systemically, there is an increase in immunosuppressive cell populations such as regulatory T cells, myeloid-derived suppressor cells (MDSCs), and M2 macrophages, which collectively enable tumor cells to evade immune surveillance and metastasize to distant organs [9]. Although immunosuppression is a hallmark of pancreatic cancer [10], investigations into immunosuppressive features of the PDAC immune landscape, especially at the systemic level using liquid biopsy, are very few. Peripheral blood mononuclear cells (PBMCs) are the immune system's first line of defense against cancer [11]. They could be a promising source of biomarkers for pancreatic cancer detection [12], as growing evidence demonstrates that systemic impairment of antitumor immunity plays a key role in the adaptive immune response in PDAC [13]. Moreover, PBMCs would not depend on tumor burden, which could be crucial for cancer detection. In this context, cutting-edge approaches such as single-cell RNA sequencing are a revolutionary tool for unraveling cellular heterogeneity and deciphering immune system dynamics, allowing the identification of disease biomarkers [14]. This technology not only facilitates the analysis of gene expression at the single-cell level but also enables the identification of gene origins across diverse cell types, thereby deepening our understanding of disease pathogenesis and clarifying the specific roles of genes and proteins in shaping the immune landscape of PDAC. In the current study, aimed at identifying liquid biopsy-based potential biomarkers that can discriminate PDAC patients from healthy subjects, we first re-analyzed single-cell transcriptomic data from PBMCs of PDAC patients and healthy controls to reveal differential gene expression and pathway activation within defined cell clusters. This analysis allowed us to identify higher expression of *S100A* family genes in the dendritic cell and monocyte populations of PDAC patients compared with healthy subjects, a finding we subsequently validated in a real-world cohort of advanced-stage PDAC patients and healthy controls.

2. Material and method

2.1. Study population

The ethical approval for this study was granted by the IRCCS Istituto Tumori "Giovanni Paolo II" of Bari under ethical code 574/2016. All participants provided informed and written consent before any procedures were conducted. The inclusion criteria for patients with pancreatic ductal adenocarcinoma included the ability to provide informed consent, being over 18 years of age, and having a histological diagnosis confirming the condition. Conversely, individuals who had undergone surgery or other treatments were excluded from the study. For healthy participants, inclusion criteria comprised being over 18 years old and capable of providing informed consent, while exclusion criteria involved the presence of inflammatory or chronic diseases. Data collection involved obtaining blood samples from patients and healthy donors prior to any surgical intervention or other treatments for the former group.

2.2. Single-cell transcriptome analysis of PBMCs

The scRNA-seq dataset, GSE155698 [13], was obtained from the Gene Expression Omnibus (GEO) and reanalyzed using the Scanpy pipeline [14–16]. This dataset contains gene expression profiles taken from PBMCs collected from 16 treatment-naïve PDAC patients, along with samples from 4 healthy donors. Initially, we employed quality control procedures to remove low-quality cells with fewer than 4000 expressed genes, more than 32,000 counts per gene, or greater than 20% mitochondrial content. Furthermore, genes expressed in only a maximum of 20 cells were removed for further analysis. The raw gene expression counts were normalized using the *sc.pp.normalize_total* function to achieve a total sum of 10^4 counts. This was followed by a logarithmic transformation to stabilize the variance. The *sc.pp.highly_variable_genes* function was applied to define Highly Variable Genes (HVGs), and the top four thousand HVGs were considered the most informative genes for further analysis. Principal component analysis (PCA) was performed on these HVGs for dimensional reduction [17,18]. The ComBat algorithm (sc.pp.combat(adata, key = 'sample')) was used to correct for batch effects within samples, with sample identity specified as the batch variable. Uniform Manifold Approximation and Projection (UMAP) was computed on the batch-corrected neighborhood graph to generate a low-dimensional visualization of the integrated dataset using `sc.tl.umap(adata)`.

The final integrated dataset comprised 34,554 cells and 18,507 genes and was used for all downstream analyses. Cell-type annotations were assigned using the CellTypist "Healthy_COVID19_PBMC" reference model, which is trained on peripheral blood mononuclear cell profiles from healthy individuals and patients with COVID-19 and comprises 51 immune cell types (version v1, released March 10, 2022). This model is well-suited to high-resolution annotation of PBMC populations and has been previously validated in large-scale immune-profiling studies [19,20]. Moreover, differential expression analysis of genes (DEGs) were identified using the *sc.tl.rank_genes_groups* function, with a paired *t*-test to identify significant gene expression differences between the PDAC and healthy groups. Genes selected for downstream analysis had an adjusted p-value <0.05 and a log2 fold change >1 or <-1. The adjusted p-values were calculated using the Benjamini-Hochberg method [21,22]. Finally, to investigate Gene Set Enrichment Analysis (GSEA), we used the WEB-based Gene Set Analysis Toolkit (webgestalt; https://www.webgestalt.org/option.php) to identify potential signaling pathways for the DEGs using Gene Ontology (GO) Biological Process gene programs. Lastly, to specifically investigate the potential disease associations of the genes of interest (*S100A6, S100A8,* and *S100A12*), we submitted them to Metascape (https://metascape.org/) for functional annotation and disease enrichment analysis using the DisGeNET database [23].

2.3. Whole blood and Peripheral blood mononuclear cells (PBMCs) isolation

A total of 10 mL of peripheral blood was collected into heparinized tubes, of which 100 μL was used for immunostaining using flow

cytometry. The remaining blood was subjected to PBMCs isolation by density gradient centrifugation using Ficoll-Hypaque, as previously described [24]. Red Blood Cells (RBCs) were lysed using ACK Lysing Buffer according to the manufacturer's protocol (Thermofisher, US). PBMCs were stored at −195 °C in media containing 20% FBS, 10% DMSO, 1% ACD, and 70% RPMI until staining.

2.4. Flow cytometry analysis (Whole blood and PBMCs)

To prevent non-specific antibody binding, the aliquots of unlysed whole blood and PBMC were first incubated with a human FcR blocking reagent (Miltenyi Biotec) following the manufacturer's instructions. Subsequently, for whole blood analysis, a surface-staining antibody cocktail — including CD3 (OKT-3), CD8 (OKT-8), CD56 (NCAM), CD25 (BC96), CD303a (201 A), CD11b (ICRF44), CD11c (3.9), CD80 (B7–1) (2D10.4), CD14 (61D3), CD83 (HB15e), CD11b (ICRF44), CD15 (MMA), HLA-DR (LN3), CD206 (MMR) and propidium iodide (10 μg/mL) was added, and samples were incubated for 30 min at 2–4 °C. Afterward, the samples were washed twice, the red blood cells were lysed using ACK buffer, and then the cells were fixed and permeabilized by Intracellular Fixation & Permeabilization Buffer Set, according to the manufacturer's instructions (ThermoScientific, #88–8823-88). The cells were incubated with an antibody cocktail for intracellular staining, FOXP3 (PCH101), IFN-γ (4S.B3), and CD68 (eBioY1/82 A (Y1/82 A)) for 30 min at room temperature, washed, and resuspended in PBS without Ca^{2+} and Mg^{2+} for acquisition.

Whole blood was used to analyze monocytes, DCs, macrophages (M1 and M2), Myeloid-derived suppressor cells (MDSCs), Treg, NKT, and $CD8^+$ T cells, according to the following gating strategy: active $CD8^+$ T cells ($CD8^+IFNg^+$), total DC ($CD11b^+CD11c^+HLADR^+$), active DC ($CD83^+CD11b^+CD11c^+HLADR^+$) plasmacytoid DC ($CD11b^+CD11c^+CD303^+$), active plasmacytoid DC ($CD83^+CD11b^+CD11c^+CD303^+$), M1 ($CD68^+HLADR^+CD80^+$), M2 ($CD68^+HLADR^+$ $CD206^+$), mMDSC ($CD11b^+HLADR^-CD14^+$), PMN-MDSC ($CD11b^+HLADR$-$CD15^+$), Treg ($CD4^+CD25^+FOXP3^+$), NKT ($CD3^+CD56^+$). The gating strategy for whole blood analysis was summarized in Supplementary Fig. 1.

The PBMCs were stained with a combination of fluorescently labeled anti-human antibodies (candidate biomarkers), including CD14 (61D3), CD86 (B7–2), CD11c (3.9), CD19 (4G7), CD83 (HB15e), CD303a (201 A), CD9 (eBioSN4), CD45RO (UCHL1), propidium iodide (10 μg/mL), and primary antibody S100A6 (3), S100A12 (161205) and S100A8 (CF-145) followed by fluorescent goat anti-mouse IgG2b and fluorescent rat anti-mouse IgG1 secondary antibodies according to a procedure based on previously described protocol [25]. PBMCs were used to analyze monocytes and DCs, and to evaluate the expression of S100A6, S100A8, and S100A12, according to the following gating strategy: monocytes ($CD14^+$), activated monocytes ($CD14^+CD86^+$), total DCs ($CD11c^+$), mature total DCs ($CD11c^+CD83^+$), plasmacytoid DCs ($CD11c^+CD303A^+$). The Attune TMNxT Acoustic Focusing Cytometer (Thermo Fisher Scientific, Waltham, MA, United States) equipped with four lasers (405 nm violet, 488 nm blue, 561 nm yellow, and 637 nm red) was used for the sample reading. The data were analyzed using the Attune TMNxT Analysis Software (Thermo Fisher Scientific, Waltham, MA, United States). The gating strategy for PBMCs was summarized in Supplementary Fig. 2. Fluorescence minus one (FMO) controls were used to define the gating boundaries for S100A proteins and to assess fluorescence compensation (Supplementary Fig. 3).

2.5. Statistical analysis

Data analysis was conducted using GraphPad Prism version 8.4.3. The Mann-Whitney *U* test was used to assess the statistical significance of mean differences between two groups (PDAC and healthy donors) in whole-blood and PBMC analyses. For the disease stages analysis, Statistical comparisons between groups (Stage II, Stage III, and Stage IV) were performed using the Kruskal-Wallis test.

A significance level of $p < 0.05$ was considered significant between the groups. "ns" indicates that the observed difference is not statistically significant (p-value >0.05); one star (*) means p-value <0.05; Two stars (**) indicate p-value <0.01, while three stars (***) represent significance with p-value <0.001. The diagnostic accuracy of $S100A^+$ immune cell populations, which differed significantly ($P < 0.05$) between PDAC patients and healthy subjects, was assessed using Receiver Operating Characteristic (ROC) analysis with an AUC ≥ 0.8.

3. Results

3.1. UMAP Visualization of PBMCs and cell distribution across the samples

Fig. 1a illustrates the workflow for processing the GSE155698 dataset. The UMAP visualizations of PBMCs from PDAC patients and healthy donors show cell distributions vary between the two groups (Figs. 1b and c). Based on the expression of gene markers using cell typist approach, the cells were categorized into 49 clusters (Fig. 1d). Notably, we observed a different distribution of immune cell clusters between healthy controls and PDAC patients, with a increased trend in myeloid populations including DCs, pDCs, and both $CD14^+$ and $CD16^+$ monocytes in the patient group, as shown in Fig. 1e. In terms of biological processes, the enrichment analyses of identified DEGs in PBMCs of the two groups demonstrated that these genes were significantly involved in processes like peptidyl-cysteine modifications, dopaminergic neuron differentiation, regulation of embryonic development, and chemokine production (FDR < 0.05) (Fig. 1f).

3.2. The S100A6, S100A8, and S100A12 mRNA expression in PBMCs

The DEG analyses have shown that *S100A6*, *S100A8*, and *S100A12* were significantly upregulated in the PBMCs of PDAC patients compared to healthy controls (adjusted p-value <0.01; Fig. 2a and Supplementary Table 1). The GeneMANIA plugin in Cytoscape 3.10.1 was used to analyze the physical interactions and co-expression of *the S100A6*, *S100A8*, and *S100A12* genes, with a maximum of 2 resultant genes. Furthermore, disease enrichment analysis using Metascape with the DisGeNET database revealed significant enrichment in pancreatic neoplasm and myocardial ischemia. These findings suggest that *S100A6, S100A8,* and *S100A12* are associated with these disease conditions, supporting their roles in inflammatory responses and cancer-related processes (Supplementary Table 1).

Based on the network result, the *S100A12* co-expressed with *advanced glycosylation end product-specific receptor* (*AGER)*, while *S100A8* co-expressed with *S100A9*. On the other side, *S100A8, S100A9, S100A12,* and *AGER* exhibit physical interactions with one another (Fig. 2b).

After identifying the *S100A6*, *S100A8*, and *S100A12* as significantly upregulated genes in the PBMCs of PDAC patients, the subsequent analyses have shown that *S100A6*, *S100A8*, and *S100A12* were expressed mainly in the monocyte and DC populations of the included PBMCs (Fig. 2c and d). Notably, there is an increasing trend in the expression of *S100A8* and *S100A12* in the monocytes and DCs of patients compared to controls (Fig. 2d).

3.3. Demographics, clinical profiles, and medical history of patients and healthy donors

A total of 19 PDAC patients and 10 healthy donors were included to validate our bioinformatic findings. These two populations were matched in terms of age and sex (Table 1). In the PDAC cohort, the majority of patients were diagnosed at the advanced stages and presented with metastases at the time of diagnosis. Only five patients underwent tumor resection (Table 1). Our validation cohort did not have patients with benign pancreatic diseases.

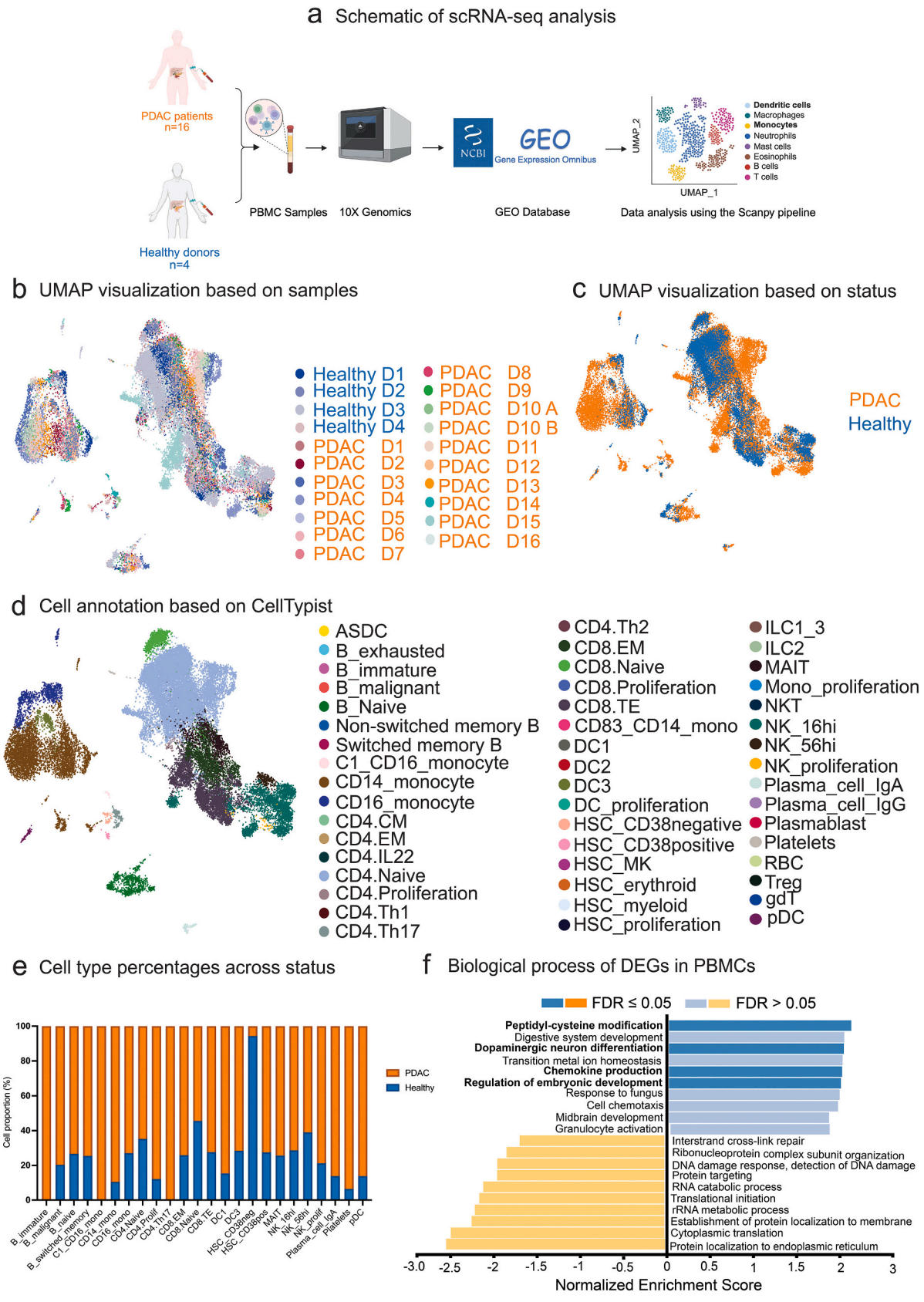

Fig. 1. Analysis of scRNA-seq data from PBMCs of PDAC patients and healthy donors. a shows the overall design of the dataset and the schematic workflow for scRNA-seq data analysis. b illustrates a UMAP visualization of cells, with colours corresponding to their respective samples. c displays a UMAP visualization of cells coloured by their status. d presents a UMAP visualization of cell types observed in PDAC and healthy samples. e displays a bar plot indicating the percentage of each cell type across different statuses. f Shows the GSEA of DEGs focusing on GO Biological Process gene programs. The Fig. 1a was designed using Biorender.

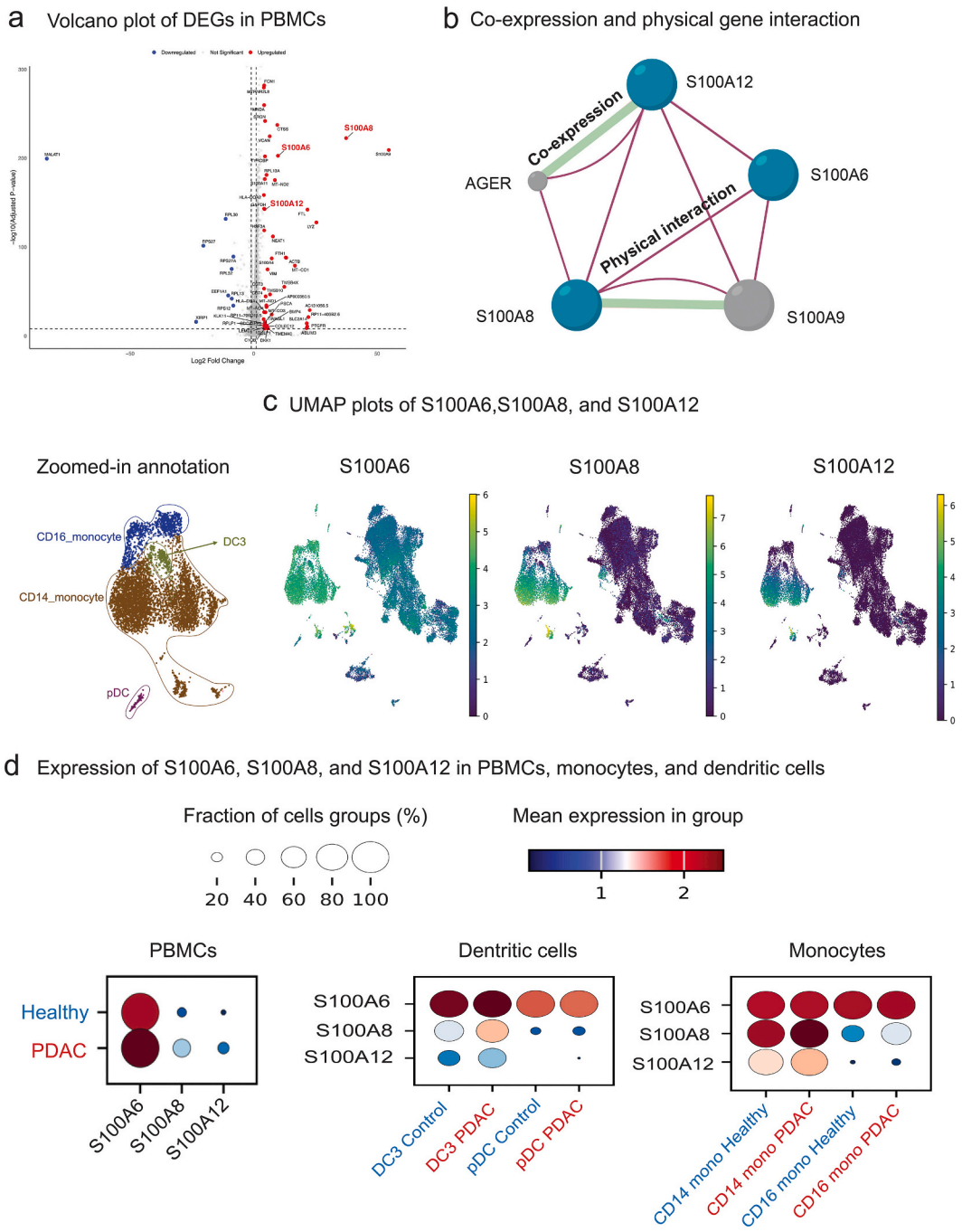

Fig. 2. Cellular and molecular characterization as well as the analysis of DEGs in PDAC PBMCs. a describes a volcano plot revealing the DEGs specific to PDAC. A cutoff (log2 fold change >4 or < −8 and adjusted *p*-value $<1 \times 10^{-8}$) was applied to highlight the most strongly regulated genes. *S100A6*, *S100A8*, and *S100A12* were considered as highly expressed genes for further investigation. b presents the analysis of co-expression/physical interaction among *S100A6*, *S100A8*, *S100A9*, *S100A12*, and *AGER* genes using the Genemania database. **c** shows a zoomed-in annotation and UMAP visualization representing the expression pattern of *S100A6*, *S100A8*, and *S100A12* genes in PBMCs, with predominant expression observed in myeloid cells (CD14_monocyte, CD_16 monocyte, pDC, and DC3). d shows a dot plot visualization of *S100A6*, *S100A8*, and *S100A12* genes in PBMCs, monocytes, and DCs.

3.4. *Immune cell changes in the whole blood of real-life cohorts of PDAC patients and controls*

We investigated the immune cell profile in intact whole blood from PDAC patients and healthy individuals to provide evidence of a comprehensive immune response in PDAC patients. As shown in Fig. 3, our analysis revealed no significant difference in monocytes and DC populations percentage between PDAC patients and healthy controls; however, some immunosuppressive cells, such as PMN-MDSCs and regulatory T cells, were higher in PDAC patients than in healthy subjects (Figs. 3i and k, respectively), while M2, M-MDSC, and plasmacytoid DC levels were not significantly different. Additionally, the M1 and activated $CD8^+$ T cell populations were significantly decreased in PDAC patients compared to healthy controls (Fig. 3f and l, respectively), suggesting that circulating immune cells are associated with a more regulatory and protumorigenic immune phenotype.

3.5. *Validation of S100A protein in the peripheral monocyte population*

To validate the *in-silico* analysis, we performed flow cytometry analysis to

Table 1
The characteristics of included PDAC patients and healthy controls.

		PDAC patients ($n = 19$) Frequency (%) or median (IQR)	Controls (n = 10) Frequency (%) or median (IQR)
Age (y)		69.8 (49–84)	60.6 (47–68)
Sex	Male	11 (57.9)	7 (70)
	Female	8 (42.1)	3 (30)
Stage at diagnosis	II	6 (31.6%)	Irrelevant
	III	3 (15.8%)	Irrelevant
	IV	10 (52.6%)	Irrelevant
Metastasis	Present	9 (47.4%)	Irrelevant
	Absent	10 (52.6%)	Irrelevant
Surgery	Yes	5 (26.3%)	Irrelevant
	No	14 (72.7%)	Irrelevant

determine how the expression of S100A6, S100A8, and S100A12 proteins differs in PBMCs of PDAC patients and healthy controls (Fig. 4a). In contrast to the in-silico data, we found that the expression of S100A6 and S100A8 proteins did not differ significantly in PBMCs from PDAC patients compared with healthy donors; additionally, the expression of S100A12 in PBMCs of patients was lower than in controls (Fig. 4b-d). To further validate the in-silico findings, we assessed the expression levels of S100A6, S100A8, and S100A12 focusing on $CD14^+$ monocyte of patient's PBMCs and compared them with those of healthy subjects. The analysis showed no significant difference in the percentage of $CD14^+$ cells in the peripheral blood of PDAC patients versus healthy controls (Fig. 4e). However, only $CD14^+$ $S100A6^+$ monocytes were significantly higher in PDAC patients than in healthy controls (Fig. 4f-h). Since Hansen et al. [26] recently found a significant increase in the expression of CD86 in circulating monocytes of PDAC patients, which are regarded as activated monocytes, we also determined the percentage of $CD86^+$ cells in the $CD14^+$ population, and we found that $CD14^+CD86^+$ monocytes were

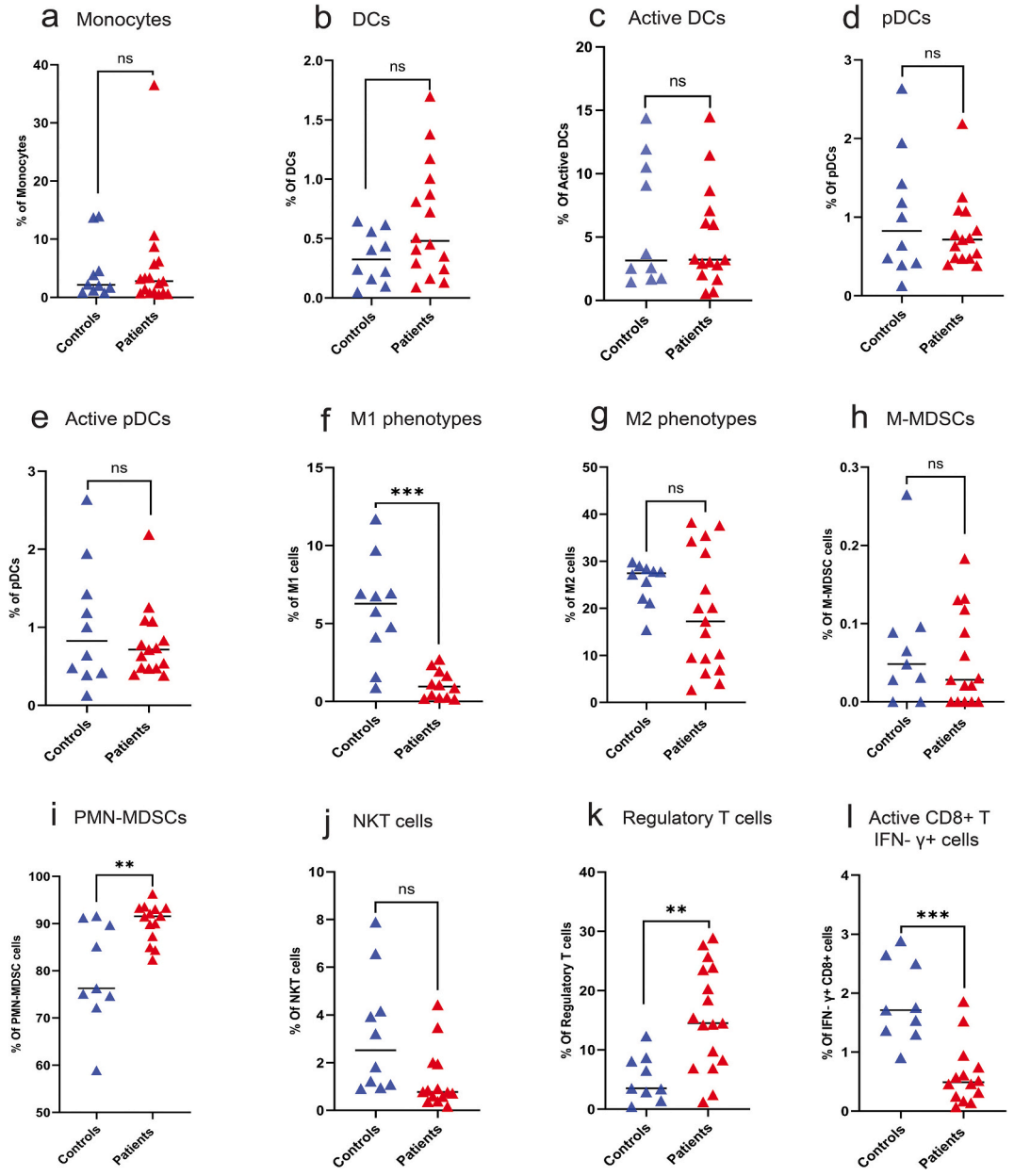

Fig. 3. Whole blood staining for immune cells. Immune populations include monocytes (a), dendritic cells (DCs) (b), activated dendritic cells (c), plasmacytoid DCs (pDCs) (d), activated pDCs (e), macrophages with both M1 (f) and M2 (g) phenotypes, myeloid-derived suppressor cells (MDSCs), including monocytic (h) and polymorphonuclear (i) subsets, natural killer T (NKT) cells (j), regulatory T cells (Tregs) (k), and IFN-γ^+ $CD8^+$ T cells (l).

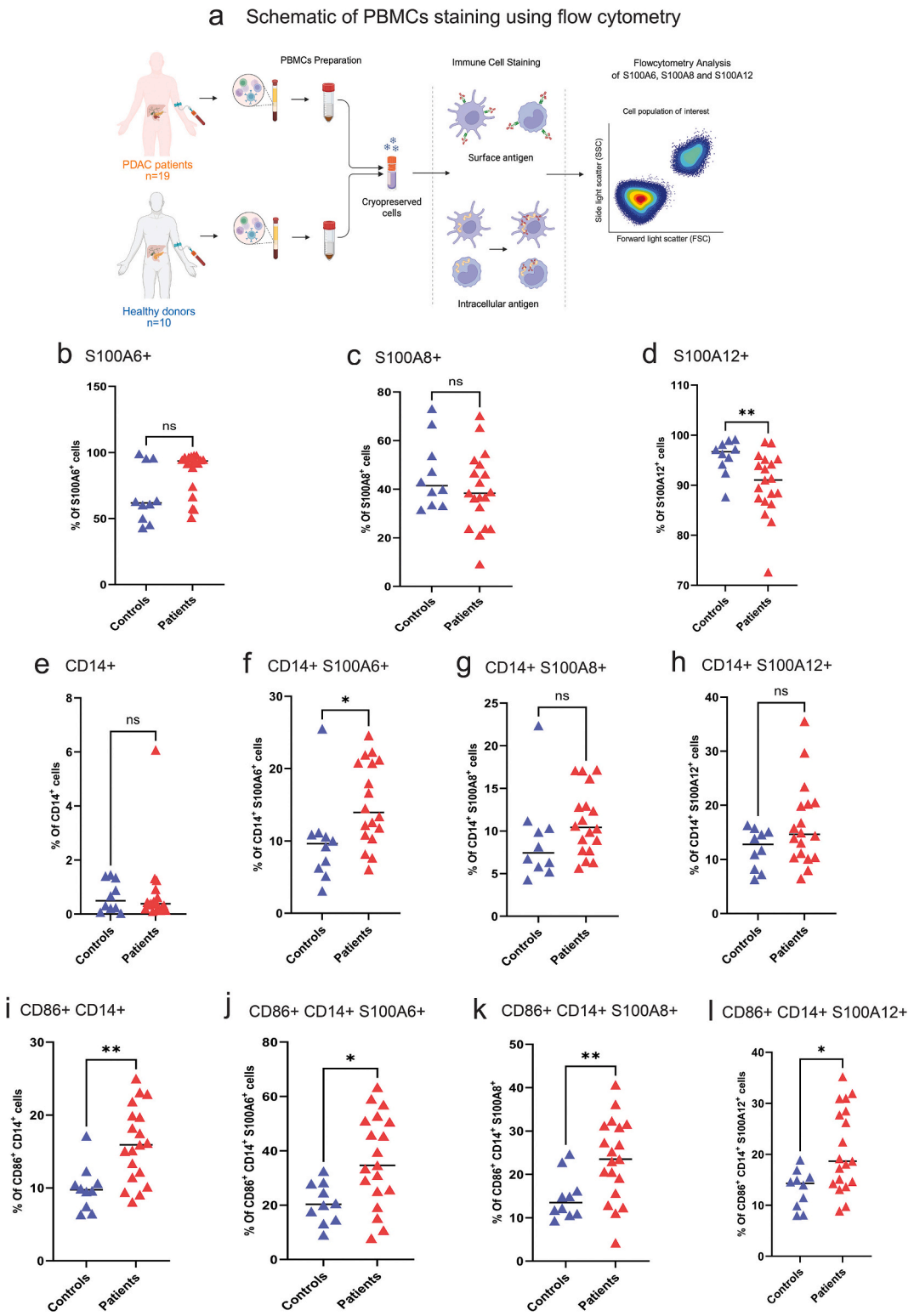

Fig. 4. Analysis of S100A6, S100A8, and S100A12 proteins in monocyte populations in PBMCs of PDAC patients and controls. Fig. 4a summarizes the process used for the flow cytometry validation of S100A6, S100A8, and S100A12 upregulation in the PBMCs of our included PDAC patients. $S100A6^+$ cells (b), $S100A8^+$ cells (c), and $S100A12^+$ cells (d), proportion of $CD14^+$ monocyte (e), $CD14^+S100A6^+$ monocytes (f), $CD14^+CD86^+S100A8^+$ monocytes (g) and $CD14^+CD86^+S100A12^+$ monocytes (h), proportion of $CD14^+CD86^+$ monocytes (i), $CD14^+CD86^+S100A6^+$ monocytes (j), $CD14^+CD86^+S100A8^+$ monocytes (k), and $CD14^+CD86^+S100A12^+$ monocytes (l).ns: not significant, $*p < 0.05$, $**p < 0.01$. Fig. 4a was designed using Biorender.

significantly higher in PDAC patients compared to healthy controls. Notably, the percentage of $CD14^+CD86^+S100A6^+$, $CD14^+CD86^+S100A8^+$, and $CD14^+CD86^+S100A12^+$ subpopulations was significantly higher in the PDAC patients compared to healthy controls (Fig. 4j-l).

3.6. Validation of the expression of S100A6, S100A8, and S100A12 in the peripheral DCs

Regarding DC populations, the results of flow cytometry analysis demonstrated that total DCs, $S100A6^+$DCs, and $S100A8^+$DCs populations were significantly higher in the PBMCs of PDAC patients than the control ones (Fig.5a-d). Accordingly, the total mature DC population, as well as the subpopulations $CD11c^+CD83^+S100A6^+$ and $CD11c^+CD83^+S100A8^+$, were significantly higher in the PBMCs of PDAC patients (Fig. 5e-h). Regarding plasmacytoid DC, our results demonstrated that total plasmacytoid DC $CD11c^+CD303A^+$ and all three plasmacytoid DC subpopulations, namely $CD11c^+CD303A^+S100A6^+$, $CD11c^+CD303^+S100A8^+$, and $CD11c^+CD303^+S100A12^+$, were significantly higher in the PBMCs of PDAC patients than controls (Fig. 5i-l).

3.7. Determination of the diagnostic value of S100A-expressing immune cell populations

We assessed the diagnostic potential of S100A-expressing immune cell populations identified in the PBMCs of patients with PDAC using ROC analysis. The association between the indicated immune cell

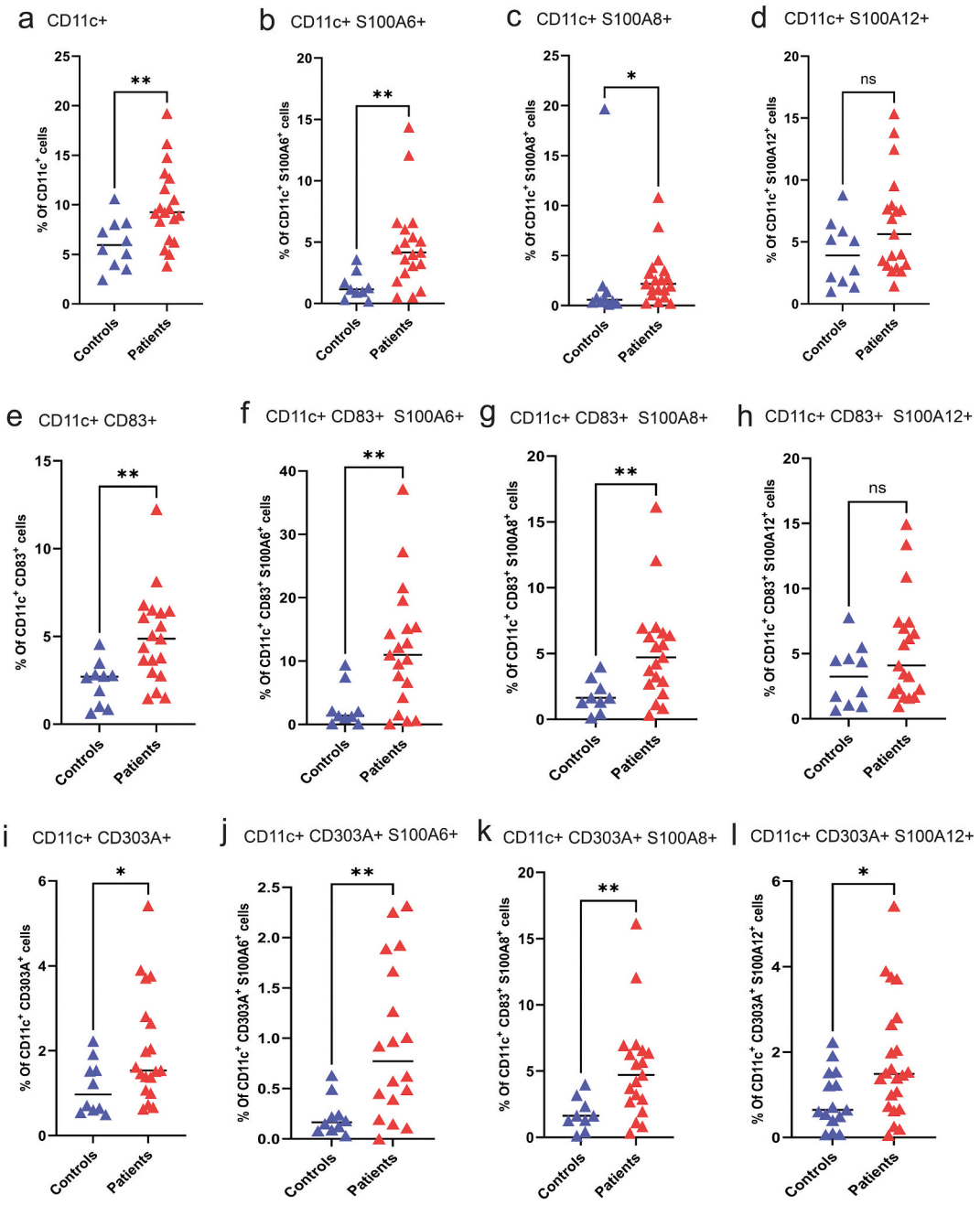

Fig. 5. Analysis of S100A6, S100A8, and S100A12 proteins in dendritic cells in PBMCs of PDAC patients and controls. (a-d) graphs showing the proportions of total DCs (a), $S100A6^+$ DCs (b), $S100A8^+$ DCs (c), and $S100A6^+$ DCs (d). (e-h) graphs illustrating the proportions of mature DC populations, including $CD11c^+CD83^+$ DCs (e), $CD11c^+CD83^+S100A6^+$ DCs (f), $CD11c^+CD83^+S100A8^+$ DCs (g), and $CD11c^+CD83^+S100A12^+$ (h). (i-l) graphs depicting the proportions of plasmacytoid DC (pDC) populations, including pDCs (i), pDCs $S100A6^+$ DCs (j pDCs $S100A8^+$ DCs (k), and pDCs $S100A12^+$ DCs (l). ns: not significant, *$p < 0.05$, and **$p < 0.01$.

populations and the presence of pancreatic cancer was assessed using AUC with 95% confidence intervals. The analysis revealed that S100A6$^+$ plasmacytoid DCs displayed an ROC curve AUC of 0.8158, S100A8$^+$ plasmacytoid DCs displayed an ROC curve AUC of 0.8447, and CD14$^+$CD86$^+$S100A8$^+$ monocytes displayed an ROC curve AUC of 0.800, ultimately showing the strongest classification performance among the evaluated immune subsets between PDAC patients and healthy subjects (Table 2). However, these represent univariate analyses only, and no combined multivariable diagnostic model was developed. The clinical applicability of these individual biomarkers requires independent prospective validation and assessment of their specificity relative to benign pancreatic diseases.

We then assessed the frequencies of these three populations across disease stages, including Stage II ($n = 3$), Stage III ($n = 6$), and Stage IV ($n = 10$) PDAC, to determine whether their abundance changes with disease progression (Supplementary Fig. 4). No statistically significant differences were observed in the frequencies of S100A6$^+$ plasmacytoid DCs, S100A8$^+$ plasmacytoid DCs, or CD14$^+$CD86$^+$S100A8$^+$ monocytes among Stage II, Stage III, and Stage IV patients. These candidate biomarkers do not appear to stratify PDAC severity across the stages assessed in this advanced-stage cohort, and their potential utility in early-stage disease detection requires further investigation.

4. Discussion and conclusion

PDAC is recognized as a highly aggressive malignancy, driven by its complex molecular profile and immunosuppressive tumor microenvironment [27]. Therefore, identifying biomarkers that distinguish PDAC patients from healthy individuals and from benign pancreatic diseases could significantly improve clinical outcomes. For this purpose, we focused on identifying systemic immune populations via liquid biopsy as potential complementary biomarkers to instrumental assessment to improve the diagnostic accuracy of the tumor. By performing the whole blood analysis of both PDAC patients and healthy donors we found a significant increase in the percentage of myeloid derived suppressor cells and regulatory T cells along with a decrease of effector cells in PDAC patients, which depicts a scenario similar to that reported by Sivakumar et al. [26], who demonstrated that circulating CD4$^+$T cells are dominated by Treg cells in PDAC patients. Overall, it correlated with reduced antitumor immune response. Since the majority of the body's immune response relies on PBMCs' activity, in order to identify critical effector molecules involved in shaping the immune landscape, and that are characteristic of patients with PDAC, we performed the in-silico analysis of differentially expressed genes in PBMCs of PDAC patients and healthy subjects, which highlighted that S100A6, S100A8, and S100A12 were significantly upregulated in DCs and the monocyte population of PDAC patients with respect to healthy subjects. The S100 protein family comprises at least 25 Ca^{2+}-binding proteins with high sequence and structural similarity [27], known to exert diverse immunomodulatory functions, such as regulation of immune cell migration, invasion, and differentiation [28–29]. Given the growing body of evidence indicating that S100 proteins play a critical role in the development and progression of various cancers, [30−31] and the established prognostic relevance of certain members, such as S100A6 and S100A8 in pancreatic cancer [32], we further investigated the expression levels of S100A6, S100A8, and S100A12 in PBMC subpopulations of real life cohort of patients with PDAC, predominantly with stage III–IV disease, compared with healthy controls.

Importantly, benign pancreatic diseases were not included in the validation cohort; therefore, the diagnostic specificity of these biomarkers, particularly their ability to distinguish PDAC from non-malignant pancreatic diseases, remains to be established in future studies.

Using flow cytometry, we found that patients with PDAC had a higher percentage of S100A6- or S100A8-positive activated dendritic cells (DCs) and plasmacytoid DCs than healthy subjects. Moreover, within the classical CD14$^+$ monocyte population, PDAC patients showed an increased proportion of activated monocytes expressing S100A6, S100A8, or S100A12, potentially reflecting a role for these proteins in modulating the adaptive immune response by promoting immunosuppressive networks that support tumor progression. Accordingly, Basso D et al. demonstrated that the S100A8/A9 soluble complex plays a role in the crosstalk between tumor cells and the immune system, ultimately suggesting that the release of these proteins allows for a progressive imbalance between regulatory and effector immune cells during pancreatic cancer progression [33]. In this context, to investigate whether the higher percentages of S100A6$^+$ plasmacytoid DCs, S100A8$^+$ plasmacytoid DCs, and CD14$^+$CD86$^+$S100A8$^+$ monocytes in PDAC patients compared to healthy subjects might have diagnostic significance, we performed ROC analysis, which revealed the highest diagnostic accuracy for all three immune cell populations. However, we acknowledge that further research is needed, particularly to elucidate the signaling pathways mediated by these S100A proteins in circulating immune cells of PDAC patients. Notably, AGER, identified by the gene-gene interaction analysis as a contributor to the functional network of S100 proteins, may play a critical role in circulating adaptive immunity, given its involvement in regulating the myeloid response in pancreatic cancer [34]. This work has several remarkable strengths and important limitations. A significant strength is that, to our knowledge, this is the first study to identify members of the S100A family at a high-resolution, cell–type–specific level in peripheral blood from patients with PDAC and to validate these findings at the protein level using flow cytometry.

Several limitations should also be acknowledged. The validation cohort was enriched for advanced-stage disease (52.6% stage IV), limiting our ability to determine whether these biomarkers perform differently in early-stage PDAC. Although stage-stratified analyses revealed no significant differences among stages II, III, and IV, the very small number of stage II cases ($n = 3$) substantially limited statistical power. Therefore, the performance of biomarkers in early-stage disease remains unresolved. Additionally, the validation cohort included only patients with PDAC and healthy controls; benign pancreatic conditions, such as pancreatitis, were not evaluated. As a result, the diagnostic specificity of these biomarkers, particularly their ability to distinguish PDAC from non-malignant pancreatic diseases, remains unknown. Third, only univariate ROC analyses were performed. No combined or multivariable diagnostic model integrating the identified biomarkers or relevant clinical variables was constructed, precluding assessment of their collective diagnostic performance and clinical readiness. Finally, while single-cell RNA sequencing enabled precise attribution of S100A6 and S100A8 expression to specific immune cell populations, additional functional and mechanistic studies are required to clarify the biological roles of S100 family proteins in PDAC-associated immune dysregulation.

Further studies using large, prospective, stage-inclusive cohorts are needed to integrate these biomarkers with clinical parameters

Table 2
The diagnostic accuracy of S100A6, S100A8, and S100A12 positive monocyte and DC sub-populations.

Population	Area under curve	CI 95%	P-value
CD14$^+$CD86$^-$S100A6$^+$ monocytes	0.7778	0.5759–0.9797	0.0165
CD14$^+$CD86$^+$S100A6$^+$ monocyte	0.7895	0.6254–0.9535	0.0116
CD14$^+$CD86$^+$S100A8$^+$ monocyte	0.8000	0.6386–0.9614	0.0089
CD14$^+$CD86$^+$S100A12$^+$ monocyte	0.7737	0.6053–0.9420	0.0170
S100A6$^+$ DCs	0.7684	0.5658–0.9710	0.0193
S100A8$^+$ DCs	0.7474	0.5400–0.9547	0.0310
S100A6$^+$ mature DCs	0.7421	0.5411–0.9431	0.0348
S100A8$^+$ mature DCs	0.7368	0.5294–0.9443	0.0389
S100A6$^+$plasmacytoid DCs	0.8158	0.6610–0.9706	0.0059
S100A8$^+$ plasmacytoid DCs	0.8447	0.6862–1.000	0.0027
S100A12$^+$ plasmacytoid DCs	0.6105	0.3818–0.8393	0.3353

(including CA 19–9), elucidate the mechanisms of S100A proteins in PDAC, and evaluate their longitudinal diagnostic, predictive, and prognostic value.

Supplementary data to this article can be found online at https://doi.org/10.1016/j.clim.2026.110665.

Preprint

Available at SSRN: https://ssrn.com/abstract=4918730

Authors' information

The authors affiliated with the IRCCS Istituto Tumori "Giovanni Paolo II", Bari, are responsible for the views expressed in this article, which do not necessarily represent the Institute.

CRediT authorship contribution statement

Afshin Derakhshani: Methodology, Data curation, Conceptualization. **Roberta Di Fonte:** Writing – review & editing, Validation, Methodology. **Letizia Porcelli:** Writing – review & editing, Methodology, Formal analysis, Data curation. **Fatemeh Nejadi Orang:** Writing – original draft. **Mahdi Abdoli Shadbad:** Writing – original draft, Methodology. **Adib Miraki Feriz:** Methodology. **Hossein Safarpour:** Methodology. **Antoine Dufour:** Writing – review & editing. **Behzad Baradaran:** Writing – review & editing. **Angela Calabrese:** Resources. **Mario Testini:** Resources. **Riccardo Memeo:** Resources. **Giovanna Di Meo:** Resources. **Leonardo Vincenti:** Resources. **Sonali Bhardwaj:** Visualization. **Vito Racanelli:** Resources. **Nicola Silvestris:** Supervision, Investigation. **Oronzo Brunetti:** Supervision, Investigation. **Amalia Azzariti:** Supervision, Investigation.

Ethics approval and consent to participate

The ethical approval for this study was granted by the IRCCS Istituto Tumori "Giovanni Paolo II" of Bari under ethical code 574/2016. All participants provided informed, written consent before any procedures were performed.

Funding

This work was supported by IRCCS Istituto Tumori "Giovanni Paolo II", Bari 5x1000 grant to O. Brunetti (Ricerca di potenziali marcatori predittivo/prognostici tissutali e circolanti in pazienti con adenocarcinoma del pancreas e delle vie biliari intra ed. extraepatiche nei setting adiuvante e metastico) and by the Italian Ministery of Health under grant to Amalia Azzariti: Ricerca Corrente 2025 - Deliberation n.197/2025 (project: Identificazione di fattori circolanti per la diagnosi, prognosi e/o predizione della risposta alle terapie in patologie tumorali solide).

Declaration of competing interest

All authors reviewed the manuscript and have declared no competing interests.

Acknowledgements

Not applicable.

Data availability

The GSE155698 dataset from GEO was re-analyzed in the current study.

References

[1] R.L. Siegel, A.N. Giaquinto, A. Jemal, Cancer statistics, 2024, CA Cancer J. Clin. 74 (2024) 12–49.
[2] J.X. Hu, C.F. Zhao, W.B. Chen, Q.C. Liu, Q.W. Li, Y.Y. Lin, F. Gao, Pancreatic cancer: a review of epidemiology, trend, and risk factors, World J. Gastroenterol. 27 (2021) 4298–4321.
[3] B.M. Flowers, H. Xu, A.S. Mulligan, K.J. Hanson, J.A. Seoane, H. Vogel, C. Curtis, L. D. Wood, L.D. Attardi, Cell of origin influences pancreatic cancer subtype, Cancer Discov. 11 (2021) 660–677.
[4] N. Sturm, T.J. Ettrich, L. Perkhofer, The impact of biomarkers in pancreatic ductal adenocarcinoma on diagnosis, surveillance and therapy, Cancers 14 (2022).
[5] W. Shi, T. Wartmann, S. Accuffi, S. Al-Madhi, A. Perrakis, C. Kahlert, A. Link, M. Venerito, V. Keitel-Anselmino, C. Bruns, Integrating a microRNA signature as a liquid biopsy-based tool for the early diagnosis and prediction of potential therapeutic targets in pancreatic cancer, Br. J. Cancer 130 (2024) 125–134.
[6] K.E. Poruk, D.Z. Gay, K. Brown, J.D. Mulvihill, K.M. Boucher, C.L. Scaife, M. A. Firpo, S.J. Mulvihill, The clinical utility of CA 19-9 in pancreatic adenocarcinoma: diagnostic and prognostic updates, Curr. Mol. Med. 13 (2013) 340–351.
[7] N.R. Nené, A. Ney, T. Nazarenko, O. Blyuss, H.E. Johnston, H.J. Whitwell, E. Sedlak, A. Gentry-Maharaj, S. Apostolidou, E. Costello, W. Greenhalf, I. Jacobs, U. Menon, J. Hsuan, S.P. Pereira, A. Zaikin, J.F. Timms, Serum biomarker-based early detection of pancreatic ductal adenocarcinomas with ensemble learning, Commun. Med. 3 (2023) 10.
[8] T. Lee, T.Z.J. Teng, V.G. Shelat, Carbohydrate antigen 19-9—tumor marker: past, present, and future, World J. Gastrointest. Surg. 12 (2020) 468.
[9] M. Muller, V. Haghnejad, M. Schaefer, G. Gauchotte, B. Caron, L. Peyrin-Biroulet, J.-P. Bronowicki, C. Neuzillet, A. Lopez, The immune landscape of human pancreatic ductal carcinoma: key players, clinical implications, and challenges, Cancers 14 (2022) 995.
[10] C. Falcomata, S. Baerthel, G. Schneider, R. Rad, M. Schmidt-Supprian, D. Saur, Context-specific determinants of the immunosuppressive tumor microenvironment in pancreatic cancer, Cancer Discov. 13 (2023) 278–297.
[11] J. Ma, Y. Lin, M. Zhan, D.L. Mann, S.A. Stass, F. Jiang, Differential miRNA expressions in peripheral blood mononuclear cells for diagnosis of lung cancer, Lab. Investig. 95 (2015) 1197–1206.
[12] E. Rodriguez, E.S. Zwart, A.A. Affandi, J. Verhoeff, M. de Kok, L.N.C. Boyd, L. L. Meijer, T.Y.S. Le Large, K. Olesek, E. Giovannetti, J.J. García-Vallejo, R. E. Mebius, Y. van Kooyk, G. Kazemier, In-depth immune profiling of peripheral blood mononuclear cells in patients with pancreatic ductal adenocarcinoma reveals discriminative immune subpopulations, Cancer Sci. 115 (2024) 2170–2183.
[13] N.G. Steele, E.S. Carpenter, S.B. Kemp, V.R. Sirihorachai, S. The, L. Delrosario, J. Lazarus, E.-A.D. Amir, V. Gunchick, C. Espinoza, Multimodal mapping of the tumor and peripheral blood immune landscape in human pancreatic cancer, Nat. Can. 1 (2020) 1097–1112.
[14] A. Miraki Feriz, F. Bahraini, A. Khosrojerdi, S. Azarkar, S.M. Sajjadi, E. Hosseinigol, M.A. Honardoost, S. Saghafi, N. Silvestris, P. Leone, Deciphering the immune landscape of head and neck squamous cell carcinoma: a single-cell transcriptomic analysis of regulatory T cell responses to PD-1 blockade therapy, PLoS One 18 (2023) e0295863.
[15] F.A. Wolf, P. Angerer, F.J. Theis, SCANPY: large-scale single-cell gene expression data analysis, Genome Biol. 19 (2018) 1–5.
[16] A. Kapilan, M. Bulluss, A.R. Ziegler, M. Dabaja, A. Derakhshani, A. Anowai, V. Armstrong, R. Campden, D. Young, Y.J. Sun, N-terminomics and proteomics analysis of Calpain-2 reveal key proteolytic processing of metabolic and cell adhesion proteins, Protein Sci. 34 (2025) e70144.
[17] N. Erfanian, S. Nasseri, A. Miraki Feriz, H. Safarpour, M.H. Namaie, Characterization of Wnt signaling pathway under treatment of lactobacillus acidophilus postbiotic in colorectal cancer using an integrated in silico and in vitro analysis, Sci. Rep. 13 (2023) 22988.
[18] A.M. Feriz, A. Khosrojerdi, M. Lotfollahi, N. Shamsaki, M. GhasemiGol, E. HosseiniGol, M. Fereidouni, M.H. Rohban, A.R. Sebzari, S. Saghafi, Single-cell RNA sequencing uncovers heterogeneous transcriptional signatures in tumor-infiltrated dendritic cells in prostate cancer, Heliyon 9 (2023).
[19] C. Domínguez Conde, C. Xu, L. Jarvis, D. Rainbow, S. Wells, T. Gomes, S. Howlett, O. Suchanek, K. Polanski, H. King, Cross-tissue immune cell analysis reveals tissue-specific features in humans, Science 376 (2022) eabl5197.
[20] E. Stephenson, G. Reynolds, R.A. Botting, F.J. Calero-Nieto, M.D. Morgan, Z. K. Tuong, K. Bach, W. Sungnak, K.B. Worlock, M. Yoshida, N. Kumasaka, K. Kania, J. Engelbert, B. Olabi, J.S. Spegarova, N.K. Wilson, N. Mende, L. Jardine, L.C. S. Gardner, I. Goh, D. Horsfall, J. McGrath, S. Webb, M.W. Mather, R.G. H. Lindeboom, E. Dann, N. Huang, K. Polanski, E. Prigmore, F. Gothe, J. Scott, R. P. Payne, K.F. Baker, A.T. Hanrath, I.C.D. Schim van der Loeff, A.S. Barr, A. Sanchez-Gonzalez, L. Bergamaschi, F. Mescia, J.L. Barnes, E. Kilich, A. de Wilton, A. Saigal, A. Saleh, S.M. Janes, C.M. Smith, N. Gopee, C. Wilson, P. Coupland, J.M. Coxhead, V.Y. Kiselev, S. van Dongen, J. Bacardit, H.W. King, S. Baker, J.R. Bradley, G. Dougan, I.G. Goodfellow, R.K. Gupta, C. Hess, N. Kingston, P.J. Lehner, N.J. Matheson, W.H. Owehand, C. Saunders, K.G. C. Smith, C. Summers, J.E.D. Thaventhiran, M. Toshner, M.P. Weekes, A. Bucke, J. Calder, L. Canna, J. Domingo, A. Elmer, S. Fuller, J. Harris, S. Hewitt, J. Kennet, S. Jose, J. Kourampa, A. Meadows, C. O'Brien, J. Price, C. Publico, R. Rastall, C. Ribeiro, J. Rowlands, V. Ruffolo, H. Tordesillas, B. Bullman, B.J. Dunmore, S. Fawke, S. Gräf, J. Hodgson, C. Huang, K. Hunter, E. Jones, E. Legchenko, C. Matara, J. Martin, C. O'Donnell, L. Pointon, N. Pond, J. Shih, R. Sutcliffe, T. Tilly, C. Treacy, Z. Tong, J. Wood, M. Wylot, A. Betancourt, G. Bower, A. De Sa,

M. Epping, O. Huhn, S. Jackson, I. Jarvis, J. Marsden, F. Nice, G. Okecha, O. Omarjee, M. Perera, N. Richoz, R. Sharma, L. Turner, E.M.D.D. De Bie, K. Bunclark, M. Josipovic, M. Mackay, A. Michael, S. Rossi, M. Selvan, S. Spencer, C. Yong, A. Ansaripour, L. Mwaura, C. Patterson, G. Polwarth, P. Polgarova, G. d. Stefano, J. Allison, H. Butcher, D. Caputo, D. Clapham-Riley, E. Dewhurst, A. Furlong, B. Graves, J. Gray, T. Ivers, M. Kasanicki, E.L. Gresley, R. Linger, S. Meloy, F. Muldoon, N. Ovington, S. Papadia, I. Phelan, H. Stark, K.E. Stirrups, P. Townsend, N. Walker, J. Webster, A.J. Rostron, A.J. Simpson, S. Hambleton, E. Laurenti, P.A. Lyons, K.B. Meyer, M.Z. Nikolić, C.J.A. Duncan, K.G.C. Smith, S. A. Teichmann, M.R. Clatworthy, J.C. Marioni, B. Göttgens, M. Haniffa, I. Cambridge Institute of Therapeutic, C.-B.C. Infectious Disease-National Institute of Health Research, Single-cell multi-omics analysis of the immune response in COVID-19, Nat. Med. 27 (2021) 904–916.

[21] M.A. Shadbad, A.M. Feriz, B. Baradaran, H. Safarpour, Tumor-infiltrating CD8+ sub-populations in primary and recurrent glioblastoma: an in-silico study, Heliyon 10 (5) (2024) e27329.

[22] H. Safarpour, J. Ranjbaran, N. Erfanian, S. Nomiri, A. Derakhshani, C. Gerarduzzi, A.M. Feriz, E. HosseiniGol, S. Saghafi, N. Silvestris, Holistic exploration of CHGA and hsa-miR-137 in colorectal cancer via multi-omic data integration, Heliyon.

[23] J. Piñero, À. Bravo, N. Queralt-Rosinach, A. Gutiérrez-Sacristán, J. Deu-Pons, E. Centeno, J. García-García, F. Sanz, L.I. Furlong, DisGeNET: a comprehensive platform integrating information on human disease-associated genes and variants, Nucleic Acids Res. (2016) gkw943.

[24] A. Derakhshani, Z. Asadzadeh, B. Baradaran, H. Safarpour, S. Rahmani, P. Leone, M. Abdoli Shadbad, N. Hosseinkhani, M. Ghasemigol, H. Ayromlou, H. Ahmadi, S. Pouya, M. Shojaee, N.J. Tabrizi, A. Miraki Feriz, E. Safarzadeh, V. Racanelli, The expression pattern of VISTA in the PBMCs of relapsing-remitting multiple sclerosis patients: a single-cell RNA sequencing-based study, Biomed. Pharmacother. 148 (2022) 112725.

[25] S. Serratì, M. Guida, R. Di Fonte, S. De Summa, S. Strippoli, R.M. Iacobazzi, A. Quarta, I. De Risi, G. Guida, A. Paradiso, Circulating extracellular vesicles expressing PD1 and PD-L1 predict response and mediate resistance to checkpoint inhibitors immunotherapy in metastatic melanoma, Mol. Cancer 21 (2022) 20.

[26] F.J. Hansen, P. David, M. Akram, S. Knoedler, A. Mittelstädt, S. Merkel, M. J. Podolska, I. Swierzy, L. Roßdeutsch, B. Klösch, Circulating monocytes serve as novel prognostic biomarker in pancreatic ductal adenocarcinoma patients, Cancers 15 (2023) 363.

[27] I.H. Sahin, G. Askan, Z.I. Hu, E.M. O'Reilly, Immunotherapy in pancreatic ductal adenocarcinoma: an emerging entity? Ann. Oncol. 28 (2017) 2950–2961.